Dye-Sensitized Solar Cells

DOI: 10.1002/anie.201103515

Tris(thiocyanate) Ruthenium(II) Sensitizers with Functionalized Dicarboxyterpyridine for Dye-Sensitized Solar Cells**

Shen-Han Yang, Kuan-Lin Wu, Yun Chi, Yi-Ming Cheng, and Pi-Tai Chou**

Dedicated to Professor Christian Bruneau on the occasion of his 60th birthday

In recent years, there has been a swift increase of research activity in ruthenium(II)-based coordination complexes as effective sensitizers in making cost-effective, third-generation photovoltaics, namely dye-sensitized solar cells (DSSCs). This activity is largely due to their lower-lying metal–ligand charge transfer (MLCT) transition that extends into the red and near-infrared region of the solar spectrum.[1] Next to the seminal **N3** and **N719** ruthenium(II) dyes, the second generation of more effective system should be credited to the anionic complex $[Bu_4N]_3[Ru(Htctpy)(NCS)_3]$ (H_3tctpy = 4,4′,4″-tricarboxy-2,2′:6,2″-terpyridine), which is known as the black dye or the **N749** dye.[2] Despite its lower absorption extinction coefficient, certified conversion efficiency of 11.1% was realized by employing a high-haze TiO_2 electrode.[3] Efforts have thus been made focusing on the enhancement of absorptivity by conducting optimization of molecular design of **N749**.[4] Parallel to this research, special attention has been paid to relevant H_3tctpy- (or Htctpy)-containing ruthenium(II) complexes, which can be readily prepared by substitution of only two thiocyanates with one bidentate heteroaromatic chelate[5] or by replacing all three thiocyanates with a single tridentate ancillary.[6] These sensitizers provide access to several respectable dye-sensitized solar cells (DSSCs), showing conversion efficiencies comparable to the best ruthenium(II) sensitizers documented in literature.

Realizing that only two carboxy groups are enough to have stable adsorption on the TiO_2 electrode,[7] herein we functionalize H_3tctpy by reducing the number of carboxy anchors on terpyridine from three to two. We then strategically incorporate a highly conjugated π-electron-donating appendage, such as thiophene, 3,4-ethylenedioxythiophene (EDOT), or functional triphenylamine, at the third carboxy-free pyridine moiety to improve the light-harvesting capability.[8] The proof of concept was then carried out by the syntheses of respective tris(thiocyanate) ruthenium(II) complexes (**PRT-11**–**14**; Scheme 1).

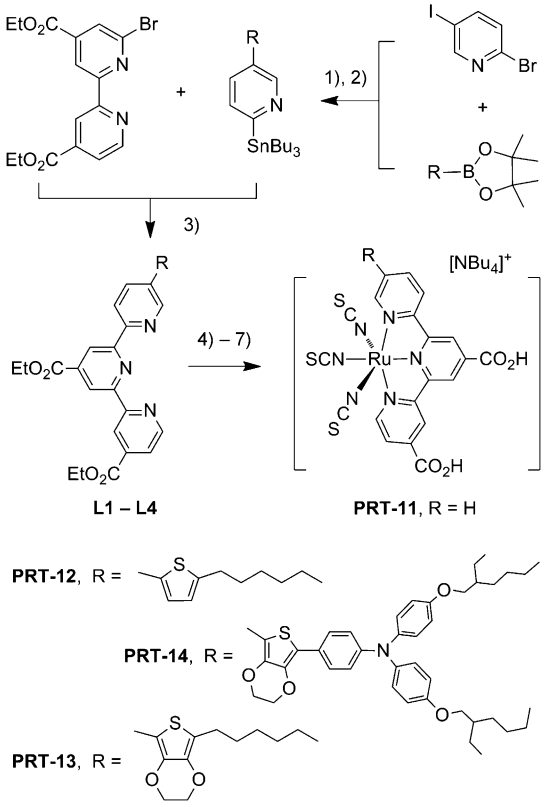

Scheme 1. Synthetic route to the functionalized Ru^{II} terpyridine sensitizers **PRT-11**–**14**; reagents and conditions: (i) $Pd(PPh_3)_4$, K_2CO_3, THF, (ii) Bu^nLi, $SnBu^n_3Cl$, −78 °C, (iii) $PdCl_2$, PBu^t_3, CuI, CsF, DMF, 80 °C, (iv) $RuCl_3$, ethanol, 90 °C, (v) $[NBu^n_4]NCS$, DMF, 145 °C, (vi) $[NBu^n_4]OH$, acetone/methanol, 60 °C, (vii) acidification to pH 2.

The targeted tridentate ligands **L1**–**L4** demand a key starting material, namely diethyl 6-bromo-2,2′-bipyridine-4,4′-dicarboxylate, which is synthesized using a modified procedure that was originally designed for the preparation of diethyl 6,6′-dibromo-2,2′-bipyridine-4,4′-dicarboxylate.[9] As shown in Scheme 1, this diethyl 6-bromo-2,2′-bipyridine-4,4′-dicarboxylate was then reacted with 2-tributylstannanyl pyridine to afford the parent chelate **L1**, that is, diethyl 4,4′-dicarboxy-2,2′:6,2″-terpyridine by Stille coupling.[10] Three more 2-tributylstannanyl pyridines were also synthesized using the rationalized procedures and subsequently applied for the preparation of thiophene-, EDOT-, and triphenylamine-functionalized chelates **L2**–**L4** (see the Supporting Information for experimental details). The ruthenium(II)

[*] S.-H. Yang, K.-L. Wu, Prof. Y. Chi, Dr. Y.-M. Cheng
Department of Chemistry, National Tsing Hua University
Hsinchu, Taiwan 30013 (R.O.C.)
E-mail: ychi@mx.nthu.edu.tw
Prof. P.-T. Chou
Department of Chemistry, National Taiwan University
Taipei, Taiwan 10617 (R.O.C.)
E-mail: chop@ntu.edu.tw

[**] This research was supported by National Science Council of Taiwan, R.O.C.

Supporting information for this article is available on the WWW under http://dx.doi.org/10.1002/anie.201103515.

complexes were then obtained from the reaction with $RuCl_3 \cdot 3H_2O$ in ethanol, followed by treatment with tetrabutylammonium thiocyanate for the anion metathesis.[11] The crude ethoxycarbonyl ruthenium(II) products were then purified by flash chromatography on silica gel. Finally, ethoxycarbonyl groups were hydrolyzed in a mixture of acetone and a 1M solution of tetrabutylammonium hydroxide in methanol. The resulting panchromatic ruthenium(II) terpyridine sensitizers **PRT-11–14** were precipitated out of the solution by adjusting the pH to 2, followed by rinsing with diethyl ether and drying in vacuo. All isolated samples were characterized by mass spectrometry and ^{1}H NMR spectroscopy (see the Supporting Information).

The absorption spectra of these **PRT** dyes are depicted in Figure 1, together with that of **N749** for a fair comparison. Their pertinent photophysical and electrochemical properties are summarized in Table 1. All **PRT** dyes have an apparent

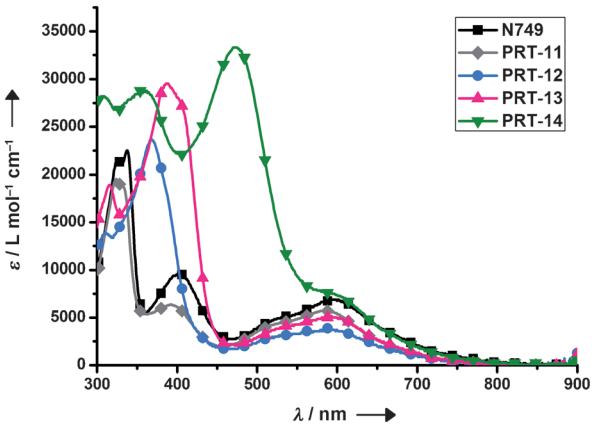

Figure 1. Absorption spectra of **N749** and **PRT-11–14** sensitizers recorded in methanol.

lowest-lying absorption band at about 600 nm, which is assigned to the MLCT transition to dicarboxy terpyridine, as a similar transition was also observed for **N749**.[2] It is notable that the intensity of MLCT band of **PRT-11** is slightly lower than that of **N749**, which is a result of the absence of the third carboxy auxochrome. This MLCT band however regains in intensity upon attachment of EDOT in **PRT-13** and especially triphenylamine in **PRT-14**, leading to a favorable hyperchromic effect that is plausibly due to the increase of donor–acceptor coupling and hence the corresponding transition dipole (see below). Moreover, except for **PRT-11**, the rest of sensitizers exhibit an intense absorption peak ranging from 350–500 nm, and the peak wavelengths are progressively red-shifted upon increasing the electron donating capability and elongating the π conjugation of the added appendage.

To gain more insight into their properties, calculations on structural optimization as well as on the electronic transitions were then carried out. Their structures were first optimized in the S_0 state with density functional theory (DFT) at B3LYP/LANL2DZ (Ru) and 6-31G* (H, C, N, O, S) level, followed by calculations of singlet electronic transitions using the time-dependent (TD) DFT method. To mimic environmental perturbation, a polarizable continuum model (PCM) was applied using dimethylformamide (DMF) as solvent.[12] The computing methods employed, together with the results of all other titled dyes, are detailed in the Supporting Information. The TDDFT results suggest that, apart for **PRT-14**, the **PRT** dyes share almost identical lowest-lying electronic transitions, of which the spin density propagation is mainly from Ru^{II} d_π orbital and occupied orbitals of thiocyanates to the antibonding orbitals of the dicarboxy terpyridine chelate. Figure 2a illustrates the calculated electronic transitions of representative **PRT-13**. A localized intraligand π–π* transition appears, as evidenced by the frontier orbital analyses and high oscillator strength, in the region of 350–480 nm, corresponding to the S_5 and/or higher excited states. For **PRT-14**, the EDOT and triphenylamine entities play a more prominent role in the intermediary transitions than that of the rest **PRT** dyes, as indicated by the greatly red-shifted and more intense transition peaks. Most interestingly, as showed in Figure 2b, the lowest-energy transition band for **PRT-14** is dominated by a intraligand π–π* transition with respectable oscillator strength ($f \approx 0.1$), confirming its increased absorptivity versus the original lower-energy MLCT. This reveals the key benefit of adding the coupled EDOT–triphenylamine chromophore.

Cyclic voltammetry was then conducted in DMF solution to verify whether their HOMO and LUMO energy levels are suitable for fabrication of DSSCs using a TiO_2 photoanode and iodide-con-

Table 1: Photophysical and electrochemical data of **PRT** sensitizers and respective DSSC parameters obtained under global AM 1.5 irradiation.

Dye	λ_{abs} [nm] (ε [L mol^{-1} cm^{-1}]) [a]	λ_{em} [nm] [a]	E°_{ox} [V] [b]	E_{LUMO} [V] [c]	TiO_2 [d]	J_{SC} [mA cm^{-2}]	V_{OC} [mV]	FF [e]	η [%]
N749	326 (21 647), 339 (22 247), 403 (9633), 522 (4816), 600 (6766)	820	0.89	−0.77	10+5	13.9	720	0.688	6.89
					15+5	16.8	720	0.707	8.54
PRT-11	324 (19 530), 393 (6375), 521 (4295), 579 (5704)	813	0.84	−0.85	10+5	13.5	680	0.733	6.75
					15+5	16.4	680	0.722	8.04
PRT-12	310 (13 931), 368 (23 697), 600 (3734)	820	0.85	−0.81	10+5	14.7	710	0.693	7.29
					15+5	17.0	750	0.715	9.10
PRT-13	316 (18 904), 389 (29 538), 535 (3987), 600 (5021)	819	0.85	−0.81	10+5	14.9	710	0.673	7.14
					15+5	19.7	760	0.686	10.3
PRT-14	309 (28 192), 362 (28 770), 475 (33 276), 600 (7394)	817	0.86	−0.80	10+5	16.3	750	0.679	8.29
					15+5	17.8	720	0.690	8.86

[a] Data were measured in MeOH solution. [b] The oxidation potential (vs. NHE) was measured in DMF with 0.1 M (nBu$_4$N)PF$_6$ and at a scan rate of 20 mVs^{-1}. It was calibrated with Fc/Fc$^+$ and converted to the NHE scale by addition of 0.63 V. [c] $E_{LUMO} = E_{ox}$-E_{0-0}, for which E_{0-0} was determined from the intersection of the absorption and tangent of the emission peak in MeOH. [d] The first and second digits indicated the thickness of 20 nm and 400 nm nanoporous TiO_2 layer in μm, respectively. [e] FF = fill factor.

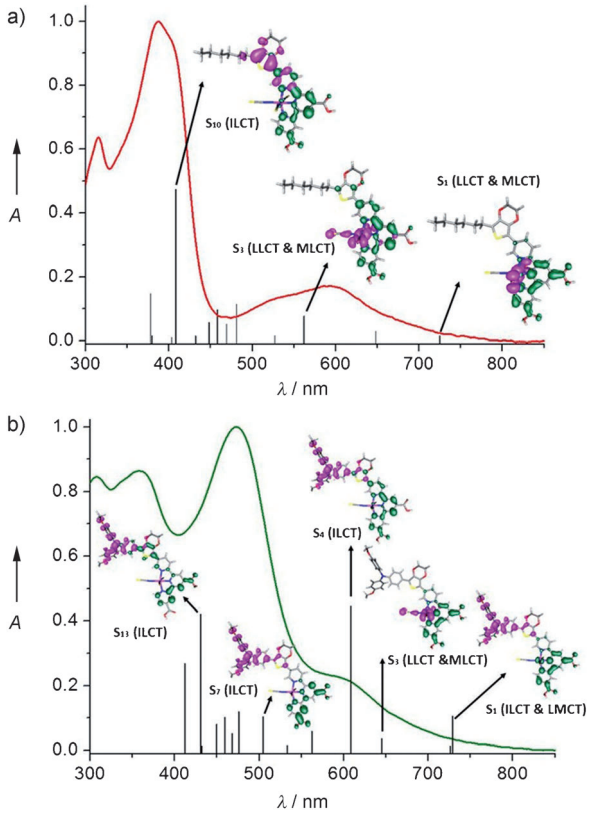

Figure 2. UV/Vis spectra and spin density plots for the specified transition of a) **PRT-13** and b) **PRT-14**. The vertical bars are pertinent optical transitions with an oscillator strength of more than 0.01, for which occupied and unoccupied orbitals are represented in magenta and green, respectively.

taining redox electrolyte. As shown in Table 1, all of their oxidation potentials appeared at about 0.85 V (vs. NHE), which are marginally lower than that of **N749** at 0.89 V and the I_2^-/I^- redox potential (< 0.93 V), but are more positive that of the I^-/I_3^- redox couple (ca. 0.4 V vs. NHE).[13] The small variation in E_{ox} of all of the complexes could be attributed to the reduced influence of the conjugated pendent of terpyridine on the ruthenium(II) metal dominated oxidation.[14] Lastly, the LUMO energy levels (ca. −0.81 V; see Table 1), estimated from the difference in the HOMO and onset of the optical energy gap E_{0-0}, are sufficiently higher than the conduction band edge of the TiO_2 electrode (ca. −0.5 V vs. NHE). Both electrochemical properties would predict rapid dye regeneration and efficient electron injection in current DSSC configurations.

The photovoltaic performance of **N749** and **PRT-11–14** on the nanocrystalline TiO_2 electrode was studied under standard AM 1.5 irradiation (100 mW cm^{-2}) using electrolytes composed of 0.6 M DMPII (dimethylpropyl imidazolium iodide), 0.5 M *tert*-butylpyridine, 0.05 M I_2, and 0.1 M LiI in acetonitrile. The short-circuit photocurrent density J_{SC}, open-circuit voltage V_{OC}, fill factors FF, and overall cell efficiencies η for each dye-TiO_2 electrode are summarized in Table 1, for which two TiO_2 layers with thicknesses of 10 + 5 and 15 + 5 μm were employed, so that their dye loading dependence on cell performance can be fairly compared.

Figure 3 a,b shows the photocurrent action spectra for the set of solar cells with TiO_2 layer thicknesses of 10 + 5 and 15 + 5 μm. The onset of the IPCE spectra are close to about 900 nm, which is the optimal parameters for anticipated best DSSCs.[15] For the first set of 10 + 5 μm devices, the **PRT-14** dye revealed the highest IPCE of 78% at 500 nm and an overall device efficiency of 8.29% (see Table 1), which is obviously due to the greater absorptivity caused by combination of triphenylamine and EDOT moieties (see above). Remarkably, upon increasing the TiO_2 thickness to 15 + 5 μm,

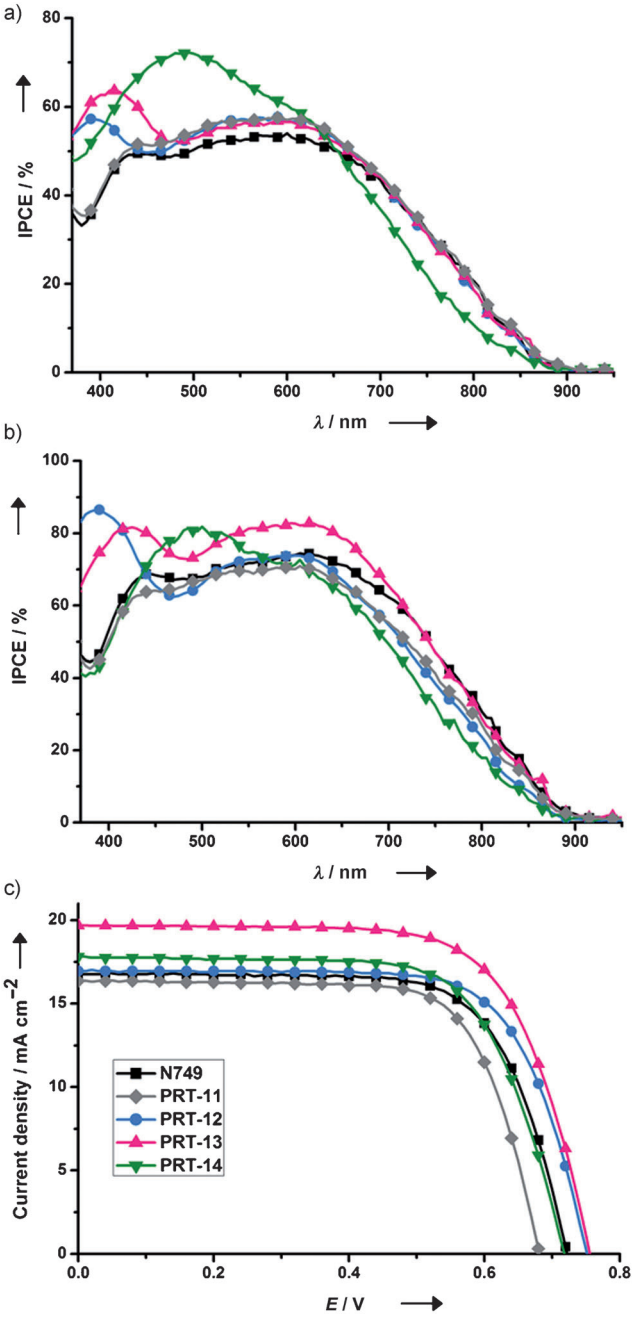

Figure 3. a) Incident photon-to-current action (IPCE) spectra of the 10 + 5 μm devices, b) IPCE spectra of the 15 + 5 μm devices, and c) current–voltage characteristics of the 15 + 5 μm devices sensitized with **N749** and various **PRT** dyes.

the **PRT-13** dye was the most efficient and showed the best IPCE of 82% at 420 nm and comparable IPCE values between 550 and 630 nm, which then produced the highest J_{SC} of 19.7 mA cm^{-2} among all DSSC devices studied herein.

Figure 3c shows the photocurrent density–voltage curve of the 15 + 5 μm devices recorded under AM 1.5G simulated sunlight at a light intensity of 100 mW cm^{-2}. In this case, the **N749** cells had $J_{SC} = 16.8$ mA cm^{-2}, $V_{OC} = 720$ mV, FF = 0.707, and $\eta = 8.54\%$. It is notable that, under similar condition, **PRT-13** dye gives $J_{SC} = 19.7$ mA cm^{-2}, $V_{OC} = 760$ mV, and FF = 0.686, corresponding to an overall conversion efficiency of $\eta = 10.3\%$. Changing from parent **PRT-11** to thiophene-anchored **PRT-12** or to EDOT-attached **PRT-13** and **PRT-14** was found to induce an increase in V_{OC} as large as 50–70 mV, indicating that the thiophene (or EDOT) unit and the associated hydrophobic carbon chain, in part, may inhibit the dark current (see below).

To gain more insight into the cell characteristics, alternating current (AC) electrochemical impedance spectroscopy was performed to analyze the effects on charge generation, transport, and collection. Typical Nyquist plots of DSSCs fabricated with all **PRT** cells in the dark under forward bias (−0.73 V) are shown in the Supporting Information, Figure S1. Two semicircles from left to right in the Nyquist plot represent the impedances of the charge transfer (R_{ct}) on the Pt counter electrode and the charge recombination (R_r) on the interface of the TiO_2/dye/electrolyte. As a result, the radius of these semicircles reveals a descending order of **PRT-13** > **PRT-12** > **PRT-14** ≈ **N749** > **PRT-11**, thus indicating that the recombination rate increases in the order **PRT-13** < **PRT-12** < **PRT-14** ≈ **N749** < **PRT-11** in the dark. This AC impedance data coincides with the trends of dark current and V_{OC} values.

We have presented a series of newly developed tris(thiocyanate) ruthenium(II) sensitizers that possess a functionalized dicarboxy terpyridine chelate. These complexes not only show better light-harvesting capabilities relative to that observed for parent **N749** in the shorter wavelength region, but also retain the characteristic MLCT transition at about 600 nm, which is necessary for improving the overall efficiencies of DSSCs. Despite the fact that the molecular design still retains all three thiocyanates, which, by conventional wisdom, were thought to be the latent photolabile moiety, the cell stability test using **PRT-13** is promising. To test this, evolution of photovoltaic parameters of **PRT-13** was measured under irradiance of AM 1.5G sunlight during visible-light soaking at 60 °C (see Supporting Information). The resulting data shown in Figure S2 reveals good stability. The device efficiency changed only from the highest recorded value of 7.96% (after 40 h) to 7.12% after 1000 h illumination, that is, a factor of 10.5% decrease. In comparison, **N749** was subject to more significant drop in J_{SC} (15%) and overall efficiency (22.2%) during the same period of irradiation. Though pending decisive explanation, one possibility of superior device stability is due to the replacement of the third carboxy group by the bulky and hydrophobic pendant, a situation relevant to the case study between **N719** and **Z907**,[16] which then prohibits the electrolyte solution to approach the sensitizer and TiO_2 surface, increasing the lifespan of the solar cells. Along this line, **RPT** dyes provide exquisite models for the comparative studies with **N749** in terms of photochemistry.

In summary, the successful preparation of sensitizers using these dicarboxy chelate opens the gateway to a brand new class of ruthenium(II)-based sensitizers that are attractive for harvesting solar irradiation up to near IR region. To further increase the photostability, the replacement of three thiocyanates with other tridentate ligands, such as 2,6-bis(5-pyrazolyl)pyridine, may offer[6] further improvement. Research focused on this is currently in progress in our laboratory.

Received: May 23, 2011
Published online: July 21, 2011

Keywords: dye-sensitized solar cells · N ligands · ruthenium · thiocyanate · thiophene

[1] a) M. Grätzel, *Acc. Chem. Res.* **2009**, *42*, 1788; b) A. Hagfeldt, G. Boschloo, L. Sun, L. Kloo, H. Pettersson, *Chem. Rev.* **2010**, *110*, 6595; c) J. Preat, D. Jacquemin, E. A. Perpete, *Energy Environ. Sci.* **2010**, *3*, 891; d) Z. Ning, Y. Fu, H. Tian, *Energy Environ. Sci.* **2010**, *3*, 1170; e) J. N. Clifford, E. Martinez-Ferrero, A. Viterisi, E. Palomares, *Chem. Soc. Rev.* **2011**, *40*, 1635; f) J.-H. Yum, E. Baranoff, S. Wenger, M. K. Nazeeruddin, M. Grätzel, *Energy Environ. Sci.* **2011**, *4*, 842.

[2] M. K. Nazeeruddin, P. Pechy, T. Renouard, S. M. Zakeeruddin, R. Humphry-Baker, P. Comte, P. Liska, L. Cevey, E. Costa, V. Shklover, L. Spiccia, G. B. Deacon, C. A. Bignozzi, M. Grätzel, *J. Am. Chem. Soc.* **2001**, *123*, 1613.

[3] Y. Chiba, A. Islam, Y. Watanabe, R. Komiya, N. Koide, L. Han, *Jpn. J. Appl. Phys.* **2006**, *45*, L638.

[4] a) K.-J. Jiang, N. Masaki, J.-B. Xia, S. Noda, S. Yanagida, *Chem. Commun.* **2006**, 2460; b) S.-R. Jang, C. Lee, H. Choi, J. J. Ko, J. Lee, R. Vittal, K.-J. Kim, *Chem. Mater.* **2006**, *18*, 5604; c) C. Lee, J.-H. Yum, H. Choi, S. O. Kang, J. Ko, R. Humphry-Baker, M. Grätzel, M. K. Nazeeruddin, *Inorg. Chem.* **2008**, *47*, 2267; d) J.-J. Kim, H. Choi, C. Kim, M.-S. Kang, H.-S. Kang, J. Ko, *Chem. Mater.* **2009**, *21*, 5719; e) Q. Yu, S. Liu, M. Zhang, N. Cai, Y. Wang, P. Wang, *J. Phys. Chem. C* **2009**, *113*, 14559; f) C.-Y. Chen, M. Wang, J.-Y. Li, N. Pootrakulchote, L. Alibabaei, C.-H. Ngoc-Le, J.-D. Decoppet, J.-H. Tsai, C. Gratzel, C.-G. Wu, S. M. Zakeeruddin, M. Grätzel, *ACS Nano* **2009**, *3*, 3103; g) W.-C. Chang, H.-S. Chen, T.-Y. Li, N.-M. Hsu, Y. S. Tingare, C.-Y. Li, Y.-C. Liu, C. Su, W.-R. Li, *Angew. Chem.* **2010**, *122*, 8337; *Angew. Chem. Int. Ed.* **2010**, *49*, 8161.

[5] a) A. Islam, H. Sugihara, M. Yanagida, K. Hara, G. Fujihashi, Y. Tachibana, R. Katoh, S. Murata, H. Arakawa, *New J. Chem.* **2002**, *26*, 966; b) A. Islam, F. A. Chowdhury, Y. Chiba, R. Komiya, N. Fuke, N. Ikeda, K. Nozaki, L. Han, *Chem. Mater.* **2006**, *18*, 5178; c) T. Funaki, M. Yanagida, N. Onozawa-Komatsuzaki, K. Kasuga, Y. Kawanishi, H. Sugihara, *Chem. Lett.* **2009**, *38*, 62; d) T. Funaki, M. Yanagida, N. Onozawa-Komatsuzaki, K. Kasuga, Y. Kawanishi, M. Kurashige, K. Sayama, H. Sugihara, *Inorg. Chem. Commun.* **2009**, *12*, 842; e) B.-S. Chen, K. Chen, Y.-H. Hong, W.-H. Liu, T.-H. Li, C.-H. Lai, P.-T. Chou, Y. Chi, G.-H. Lee, *Chem. Commun.* **2009**, 5844.

[6] C.-C. Chou, K.-L. Wu, Y. Chi, W.-P. Hu, S. J. Yu, G.-H. Lee, C.-L. Lin, P.-T. Chou, *Angew. Chem.* **2011**, *123*, 2102; *Angew. Chem. Int. Ed.* **2011**, *50*, 2054.

[7] a) M. K. Nazeeruddin, R. Humphry-Baker, P. Liska, M. Grätzel, *J. Phys. Chem. B* **2003**, *107*, 8981; b) P. Chen, J. H. Yum, F. De Angelis, E. Mosconi, S. Fantacci, S.-J. Moon, R. H. Baker, J. Ko, M. K. Nazeeruddin, M. Grätzel, *Nano Lett.* **2009**, *9*, 2487;

c) K. Chen, Y.-H. Hong, Y. Chi, W.-H. Liu, B.-S. Chen, P.-T. Chou, *J. Mater. Chem.* **2009**, *19*, 5329; d) F. De Angelis, S. Fantacci, A. Selloni, M. K. Nazeeruddin, M. Grätzel, *J. Phys. Chem. C* **2010**, *114*, 6054.

[8] a) W.-H. Liu, I.-C. Wu, C.-H. Lai, C.-H. Lai, P.-T. Chou, Y.-T. Li, C.-L. Chen, Y.-Y. Hsu, Y. Chi, *Chem. Commun.* **2008**, 5152; b) R. Li, X. Lv, D. Shi, D. Zhou, Y. Cheng, G. Zhang, P. Wang, *J. Phys. Chem. C* **2009**, *113*, 7469; c) W. Zeng, Y. Cao, Y. Bai, Y. Wang, Y. Shi, M. Zhang, F. Wang, C. Pan, P. Wang, *Chem. Mater.* **2010**, *22*, 1915; d) M. Wang, S.-J. Moon, D. Zhou, F. Le Formal, N.-L. Cevey-Ha, R. Humphry-Baker, C. Graetzel, P. Wang, S. M. Zakeeruddin, M. Grätzel, *Adv. Funct. Mater.* **2010**, *20*, 1821.

[9] C. Barolo, M. K. Nazeeruddin, S. Fantacci, D. Di Censo, P. Comte, P. Liska, G. Viscardi, P. Quagliotto, F. De Angelis, S. Ito, M. Grätzel, *Inorg. Chem.* **2006**, *45*, 4642.

[10] a) A. Puglisi, M. Benaglia, G. Roncan, *Eur. J. Org. Chem.* **2003**, 1552; b) S. P. H. Mee, V. Lee, J. E. Baldwin, *Chem. Eur. J.* **2005**, *11*, 3294.

[11] H.-J. Park, K. H. Kim, S. Y. Choi, H.-M. Kim, W. I. Lee, Y. K. Kang, Y. K. Chung, *Inorg. Chem.* **2010**, *49*, 7340.

[12] a) S. Ghosh, G. K. Chaitanya, K. Bhanuprakas, M. K. Nazeeruddin, M. Grätzel, P. Y. Reddy, *Inorg. Chem.* **2006**, *45*, 7600; b) M.-X. Li, X. Zhou, B.-H. Xia, H.-X. Zhang, Q.-J. Pan, T. Liu, H.-G. Fu, C.-C. Sun, *Inorg. Chem.* **2008**, *47*, 2312; c) E. S. Böes, P. R. Livottoa, H. Stassen, *Chem. Phys.* **2006**, *331*, 142.

[13] G. Boschloo, A. Hagfeldt, *Acc. Chem. Res.* **2009**, *42*, 1819.

[14] a) P.-T. Chou, Y. Chi, *Chem. Eur. J.* **2007**, *13*, 380; b) Y. Chi, P.-T. Chou, *Chem. Soc. Rev.* **2007**, *36*, 1421.

[15] H. J. Snaith, *Adv. Funct. Mater.* **2010**, *20*, 13.

[16] a) P. Wang, S. M. Zakeeruddin, J. E. Moser, M. K. Nazeeruddin, T. Sekiguchi, M. Grätzel, *Nat. Mater.* **2003**, *2*, 402; b) P. Wang, S. M. Zakeeruddin, R. Humphry-Baker, J. E. Moser, M. Grätzel, *Adv. Mater.* **2003**, *15*, 2101.

